Proc. Natl. Acad. Sci. USA
Vol. 74, No. 2, pp. 477–481, February 1977
Biochemistry

Heteroduplex analysis of avian RNA tumor viruses

(RNA·DNA hybrids/Rous sarcoma virus/transformation defective virus/virus replication model/glyoxal denaturation)

R. P. JUNGHANS*†, S. HU‡§, C. A. KNIGHT*, AND N. DAVIDSON‡

* Department of Molecular Biology and Virus Laboratory, University of California, Berkeley, Calif. 94720; and ‡ Department of Chemistry, California Institute of Technology, Pasadena, Calif. 91125

Contributed by Norman Davidson, November 8, 1976

ABSTRACT **Electron microscopic heteroduplex analysis of avian RNA tumor viruses has been undertaken by using 35S viral RNA and long, complementary DNA synthesized *in vitro*. In this initial study, heteroduplex molecules were formed between complementary DNA from Rous sarcoma virus [Prague B strain (Pr-B)] and RNAs from Pr-B and Rous sarcoma virus [Prague C strain (Pr-C)] and from their transformation defective (*td*) derivatives, td-Pr-B and td-Pr-C. In the case of heteroduplexes with the *td* viruses, a deletion loop was observed of the order of two kilobases in size and less than one kilobase from the 3′ terminus of the RNA. This deletion probably spans part or all of the sequences of one or more genes in the nondefective sarcoma virus which are essential for cell transformation. The sizes and the positions of the deletions in the td-Pr-B and td-Pr-C viruses were slightly, but significantly, different. No nonhomology features were observed in the Pr-B·Pr-C hybrids, thus confirming the close genetic relatedness of the two viruses.**

All heteroduplexes contained a proportion of circular and dimer molecules. This observation is a direct demonstration that (−) strand DNA transcription begins at an internal position of the RNA genome, proceeds to the 5′ end, reinitiates at the 3′ end of the RNA, and copies the remainder of the viral genome. Other implications for models of RNA tumor virus replication are also developed from these data.

Electron microscope heteroduplex analysis is a method for detecting and mapping regions of sequence homology and nonhomology between related nucleic acid species (1). The correlation of the results of heteroduplex analysis with genetic differences between the sources of the nucleic acids permits construction of a partial or complete physical gene map.

The genomes of RNA tumor viruses have not been directly amenable to heteroduplex studies since the viral RNA is single stranded. Attempts to synthesize complementary DNA (cDNA) *in vitro* have in the past yielded only products which were very short (2); whereas for the heteroduplex method to be practical, it is helpful, if not essential, that the cDNA transcripts be comparable in size to the viral RNA. Progress has recently been made in the synthesis of full size DNA transcripts of tumor virus RNA (3), thus overcoming this obstacle to heteroduplex analysis. We present here the first successful application of this general approach to the investigation of RNA tumor virus genomes.

MATERIALS AND METHODS

Viral Nucleic Acids. Cloned stocks of Rous sarcoma virus [Prague B strain (Pr-B)], transformation defective Prague B strain (td-Pr-B), and an uncloned stock of Prague C strain were used. Viruses were grown and purified and nucleic acids prepared according to published procedures (3, 4).

Hybridization. Hybridizations were performed in volumes of 10–20 μl in sealed glass capillaries containing from 50 to 200 ng of total nucleic acid with either the DNA or the RNA in a 2- to 4-fold mass excess. Annealing conditions were either 1 M NaOAc buffer at pH 6.1, or 1 M NaCl/0.04 M ($NaPO_4$ buffer at pH 7.0 and temperature at 52°; incubations were generally conducted for 3–20 hr.

These annealing conditions were selected to minimize degradation of nucleic acids during hybridization reactions while permitting hybrid formation to take place, albeit at a diminished rate (5). With the annealing conditions used, both RNA and single-stranded DNA of 3×10^6 daltons were stable for up to 50 hr. The use of formamide at 50% (vol/vol) concentration in these hybridizations led to significant degradation of both single-stranded DNA and RNA of this size for incubations longer than about 4–8 hr at 52°, and use of aqueous conditions at higher temperatures (68°) degraded the RNA in incubations of 2 hr or longer (R. Junghans, unpublished).

Electron Microscopy. Hybrids were treated with 1 M glyoxal in 0.01 M (Na)PO_4 buffer at pH 7.0 for 1 hr at 37° and the poly(A) mapping technique (6) was applied to determine hybrid polarity. Simian virus (SV)40-poly(dT) was a gift of W. Bender. SV40 DNA was included in all spreads as an internal length standard. The length of SV40 double-stranded, relaxed circular DNA, for which we assume a polynucleotide length of 5.55 kilobases (kb), was measured as 1.76 ± 0.06 μm. A double-strand to single-strand length ratio of 1.24 was established with φX174 double-stranded and single-stranded circular standards.

RESULTS

Homoduplex Studies between Pr-B RNA and Pr-B DNA. Hybrid molecules were formed between Pr-B RNA and Pr-B cDNA. The cDNA had been fractionated on alkaline sucrose gradients to a size of $\geq 2.5 \times 10^6$ daltons, approximating the length of the viral genome (3). Among the hybrids the following structures were seen by electron microscopy: (*i*) linear molecules of monomer RSV genome length (Fig. 1a), (*ii*) circular molecules of monomer length (Fig. 1b and c), and (*iii*) linear dimer molecules (Fig. 1d and e). The linear hybrid molecule of Fig. 1a is distinguished only in terms of qualitative features from an unhybridized, single-stranded RNA molecule; the greater thickness and evenness of texture and the extended configuration are characteristic of duplex regions. Neither DNA nor RNA by themselves showed circular or dimer structures.

With conditions of hybridization in DNA excess, multiple nucleations of DNA on the RNA were sometimes observed. Fig. 1e shows a heteroduplex with long single-stranded DNA tails where two DNA molecules meet on the same RNA molecule. These molecules could be produced when two DNAs hybridize simultaneously to the same RNA molecule, or when the DNA or RNA in the initial hybrid is shorter than full genome length and leaves a single-strand gap where another RNA or DNA can

Abbreviations: cDNA, complementary DNA; PR-B, Rous sarcoma virus Prague B strain; PR-C, Rous sarcoma virus Prague C strain; SV40, simian virus 40; kb, kilobases; *td*, transformation defective.

† Present address: Department of Chemistry 164-30, California Institute of Technology, Pasadena, Calif. 91125.

§ Present address: Department of Microbiology, University of Southern California Medical Center, Los Angeles, Calif. 90033.

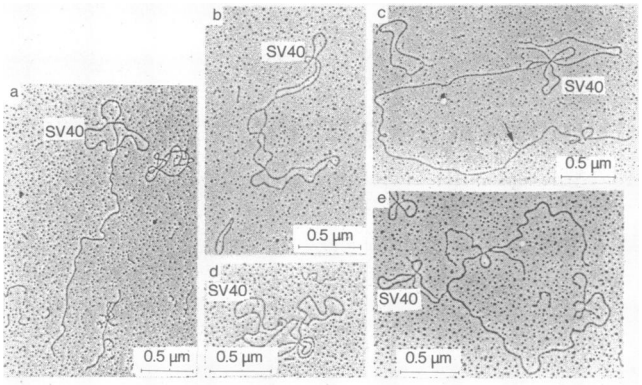

FIG. 1. DNA·RNA heteroduplex structures. (a) Pr-B·Pr-B linear hybrid of monomer length with SV40 attached. (b) Pr-B·Pr-C circular hybrid of monomer length with SV40 attached. (c) Pr-B·Pr-B circular hybrid of monomer length with SV40 attached. (d) Pr-B·Pr-B linear dimer with SV40 attached at the end. From SV40 to the small tail (arrow) is approximately unit genome length; the second molecule is broken and is only 60% of the unit genome length. The tail is about 200 nucleotides in length and presumably represents the poly(A) tail of the second RNA molecule (see Fig. 2). (e) Pr-B·Pr-B linear dimer with SV40 attached at the middle of the structure. The lower arm of the dimer is unit genome length; the upper arm is 0.6 genome length and apparently has two DNA molecules hybridized to it.

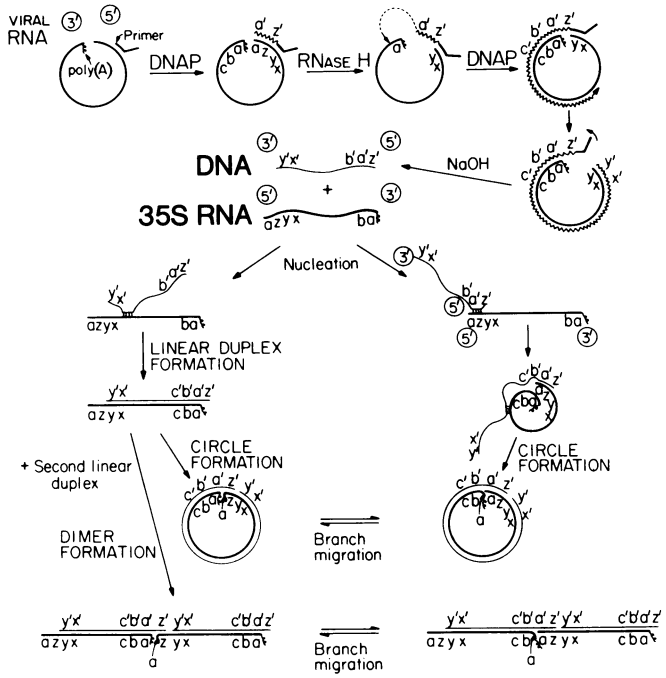

FIG. 2. Replication model and mechanism of formation of observed heteroduplex structures. The replication model is represented as follows. The tRNA 4S primer is located near the 5′ end of the genome (16). DNA transcription (DNAP) proceeds from this point, copying first a sequence (*z*) which is uniquely represented at the 5′ end of the genome and then a sequence (*a*) which is repeated at the 3′ end of the genome. When transcription reaches the 5′ end, the RNA terminus is then in DNA·RNA hybrid form, and RNase H acts on the RNA to digest it from the 3′ terminus of the newly synthesized DNA. [RNase H is a 3′ → 5′ and 5′ → 3′ exonuclease which digests RNA from DNA·RNA hybrids to generate 3′ OH RNA fragments of 2 to 12 nucleotides in length (9, 10). The enzyme does not act unless and until the RNA terminus is itself complexed with a complementary DNA strand (9).] This single-stranded DNA is then complementary at its 3′ end to the terminally repeated segment at the 3′ end of the RNA with which the short DNA is now free to associate, and the molecule becomes circular. At this stage, DNA synthesis resumes and the remainder of the RNA is transcribed, until the primer is displaced and a linear duplex structure is generated. The rest of the model for *in vivo* replication (not shown) postulates that RNase H activity on this new DNA·RNA terminus at the 5′ end of the RNA generates new RNA fragments, one or more of which serve as primer for DNA-dependent DNA synthesis to copy the (−) strand DNA into a DNA duplex structure. By the action of RNase H and/or cellular enzymes, the circle is trimmed of remaining RNAs which served as primers for each direction of DNA synthesis; sticky ends are generated on the DNA and the molecule circularizes. [If the tRNA primer for the first (RNA → DNA) round of transcription is itself copied into DNA at the end of the second (DNA → DNA) round of transcription, a single-strand DNA tail will be attached to the duplex circle and must also be removed by cellular enzymes.] Any remaining short single-strand gaps are filled by viral or cellular DNA polymerase, and the molecule finally is ligated into a covalently closed duplex circle and integrated into the cellular genome.

In the diagram, the DNA product of the first (RNA → DNA) round of transcription is annealed to intact viral 35S RNA. This annealing is represented as taking place via two alternate pathways. By the first (left-hand) pathway, molecules with sticky ends are formed to yield linear monomers, circular monomers, or linear dimers as shown. (Linear dimers may also form by other pathways not shown.) The second (right-hand) pathway yields only circular molecules. Circles and dimers with alternative positionings of the terminally redundant sequences, *a*, are interconvertible by branch migration between the 3′ and 5′ RNA termini in the hybrids.

anneal. In either case, the DNAs or RNAs would then be free to branch-migrate (7) in the hybrid to yield crossed structures like that in the upper arm of the hybrid in Fig. 1e. If short DNA molecules were used in the hybridization (0.2–0.5 × 10^6 daltons), then this problem was exaggerated. Very complex branched structures were commonly observed, attributable to multiple DNA nucleations on the same RNA and as well as to further DNA nucleations on the DNA itself. While the large DNA (≥2.5 × 10^6 daltons) molecules synthesized *in vitro* and isolated on alkaline sucrose gradients are greater than 98% of (−) strand polarity, the smaller molecules of 2 × 10^6 down to 10^5 daltons are from 10 to 50% (+) strand, respectively (3, 8). Circular molecules were sometimes observed among DNA·RNA hybrids with these short DNA molecules as well (not shown).

Fig. 2 depicts a model for the formation of the cDNA transcript and shows pathways for the hybridization reaction leading to linear and circular monomer and linear dimer heteroduplex molecules. This model is described in more detail in the legend and in the *Discussion* section.

Length measurements were made on circular Pr-B RNA·Pr-B cDNA homoduplexes, because, according to the model in Fig. 2, circularity ensures that the molecule is fully unit genome in length. Measurements of 20 molecules gave a mean length of 9.50 ± 0.57 kb. By adding 0.20 kb for the poly(A) length at the 3′ end of the RNA (11) we calculate an overall chain length of 9.70 ± 0.57 kb (Fig. 3).

Heteroduplex Studies. The transformation defective (*td*) viruses arise as spontaneous segregants from tumor virus stocks (12). As discussed below, previous studies by other techniques have suggested that these viruses are simple deletion mutants of the nondefective parental sarcoma viruses, and this is confirmed by the present heteroduplex studies. Heteroduplex molecules were formed between Pr-B DNA and RNA from a *td* mutant of the same strain, td-Pr-B. These hybrids displayed the linear monomer, linear dimer, and circular monomer structures seen in the homoduplex Pr-B·Pr-B case. In addition, a deletion loop was observed near the 3′ end of the RNA. No other reproducible nonhomology features were seen in these heteroduplexes. Fig. 4a and b shows linear monomer and circular monomer structures with such deletion loops. In measurements of 44 molecules, the distance from the 3′ end of the

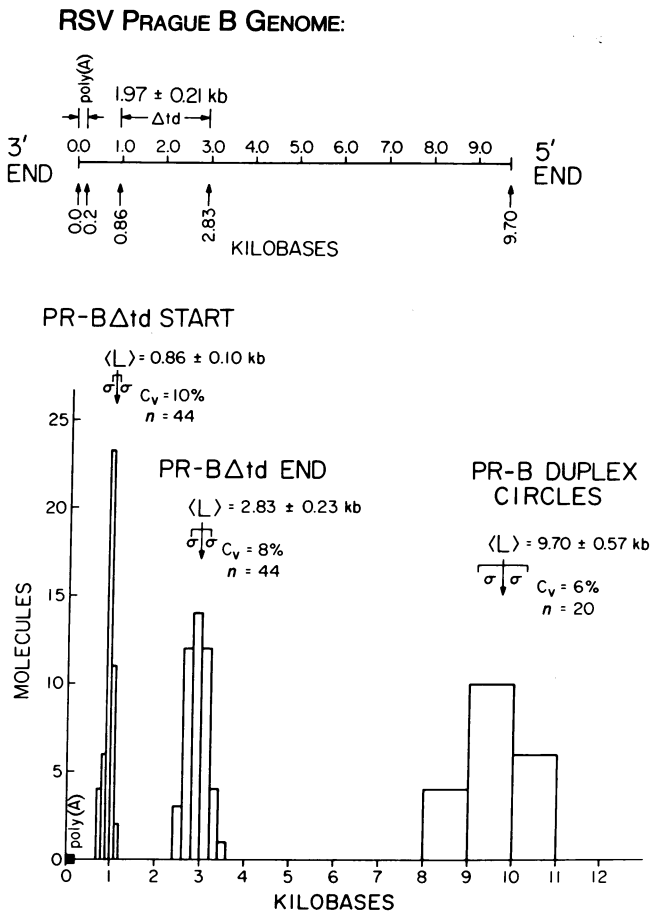

FIG. 3. Histograms of lengths of Pr-B-Pr-B homoduplex circles, positions of deletion loops in Pr-B-td-Pr-B heteroduplexes, and a summary map deduced from these data. Molecules were measured and converted to units of kilobases (1000 nucleotides) according to double-strand and single-strand size standards (see *Materials and Methods*).

RNA to the site of the loop was 0.86 ± 0.10 kb and the length of the loop was 1.97 ± 0.21 kb (Fig. 3).

The Pr-B virus used in the experiments reported here was from a recently cloned stock, and showed only large 35S ["a" class (ref. 13)] subunits on gel electrophoresis (not shown), as expected for pure, nondefective sarcoma virus (13). However, a very small fraction (<1%) of the Pr-B-Pr-B homoduplexes also showed deletion loops, apparently representing a small subpopulation of newly arisen transformation defective segregants.

Pr-C is another member of the Prague Rous sarcoma virus group, with a host range on chicken cells that differs from that of the Pr-B strain (14). Heteroduplex studies between Pr-B DNA and Pr-C RNA were performed, and no regions of nonhomology were detected among the hybrids (Fig. 1b).

The stock of Pr-C used was a laboratory strain which was not cloned recently, and a large number of molecules with deletion loops typical of the Pr-B-td-Pr-B hybrids was seen among the Pr-B-Pr-C hybrids (not shown). In 24 molecules, the deletion began at 0.73 ± 0.21 kb from the 3′ end of the RNA and extended to 3.11 ± 0.34 kb, resulting in an overall deletion size of 2.38 ± 0.27 kb. The size and the beginning and ending positions of the deletion were different from those of the td-Pr-B virus all at significance levels of $\alpha < 0.001$ by a two-tailed Student's *t*-test. The td-Pr-C deletion begins approximately 130 ± 34 nucleotides closer to the 3′ end of the RNA genome and

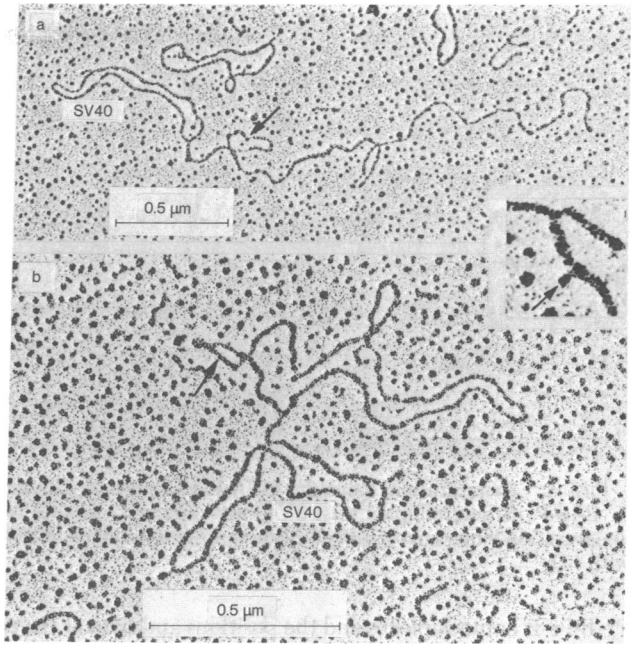

FIG. 4. Pr-B-td-Pr-B heteroduplexes. (a) Linear hybrid with SV40 attached with *td* deletion loop (arrow) which occurs reproducibly in this position. The second loop is a random crossover in the hybrid. (b) Circular hybrid with SV40 attached with *td* deletion loop (arrow). Inset: blow-up of "tab" (arrow) near SV40 in a linear hybrid. A similar "tab" is also seen at the corresponding position in the hybrid in (a).

ends about 280 ± 75 nucleotides farther from the 3′ end of the genome than the td-Pr-B deletions, thereby yielding a td-Pr-C deletion larger overall by about 410 ± 65 nucleotides.

As a final note on the *td* studies, it is necessary to explain a correction we have applied to some of the data. The length of the poly(dT) tails on the SV40 molecules was measured as 195 ± 59 nucleotides ($n = 74$). Poly(A) on RSV is known to be close to 200 nucleotides in length (11). If the poly(A) and poly(dT) tracts match up perfectly in the poly(A) mapping, then the distance from SV40 to the heteropolymeric sequences in the RSV RNA should be about 200 nucleotides. However, this distance was measured to be 292 ± 77 nucleotides ($n = 58$), which is different from the mean expected distance of 200 nucleotides at a significance level of $\alpha < 0.001$. To make this measurement, we determined the distance from the SV40 circles to the point of junction of the poly(A) with RSV circles, broken circles, or dimers (see Fig. 2). We assume this average discrepancy of 100 nucleotides in length is due to slippage in the poly(A)-poly(dT) hybrids, which we suppose occurs as a consequence of stretching forces in the cytochrome monofilm during the spreading procedure. The numbers for the distances from the 3′ end of the RNA to the positions of the *td* loops are reported as 0.1 kb less than those calculated from our direct measurements to reflect a correction for this postulated slippage.

Denatured Regions Observed in DNA-RNA Hybrids. A problem was encountered which may be of general interest in heteroduplex studies which use glyoxal treatment to maintain single-stranded regions in extended conformation during low formamide spreading conditions. Denatured regions were observed in hybrids with variable, but sometimes significant (>10%), frequency. Fig. 5 shows an example of a Pr-B-td-Pr-B heteroduplex with denaturation regions in addition to the expected deletion loop. The denatured regions do not represent nonhomology regions because such regions appeared in

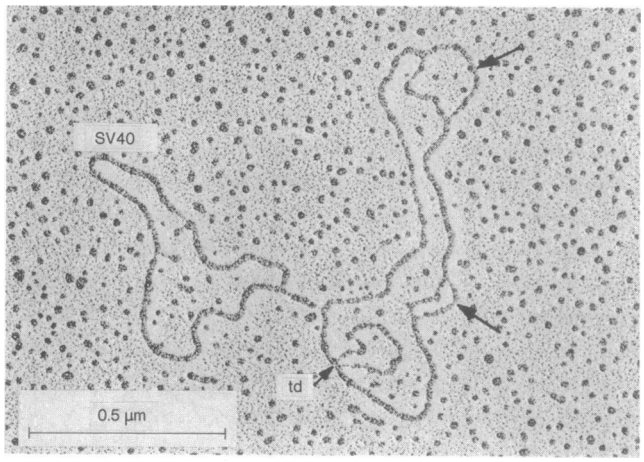

FIG. 5. Denaturation loops in DNA·RNA hybrids. Circular Pr-B·td-Pr-B heteroduplex with SV40 attached and showing two denaturation loops (arrows) in addition to *td* deletion loop (arrows with *td*).

Pr-B·Pr-B homoduplexes and the positions and sizes of the regions were random.

The glyoxal incubation under low salt conditions was suspected as the source of the denaturation. This hypothesis was confirmed in a test in which 0.1 M NaCl was added to the standard glyoxal incubation (*Materials and Methods*) to stabilize duplex regions; under these conditions, the occurrence of denatured regions was markedly reduced. Moreover, such regions disappeared virtually completely when hybrids were spread in the mildly denaturing 60% urea plus formamide (U+F) solvent (15) without prior glyoxal treatment (data not shown; and Y. Chien, personal communication).

DISCUSSION

The observation of circular and dimer structures among the hybrids is direct, positive evidence that transcription begins at an internal position of the RNA, proceeds to the 5′ end, reinitiates at the 3′ end of the RNA, and copies the remainder of the viral genome. Because circles were also observed when short DNAs of 2 to 5×10^5 daltons were used in the hybridization, it can probably be inferred as well that the site of initiation of DNA synthesis is close to the 5′ end of the 35S RNA. Although it has been shown previously that a 4S primer for DNA synthesis is located near the 5′ end of the viral genome (16), the data presented here are the first direct demonstration that transcription of 3′ end and other internal RNA sequences into DNA can also initiate from this site. The gap between the 5′ and 3′ termini of the viral RNA is somehow bridged to yield a single DNA polynucleotide chain transcript containing 5′ end and 3′ end RNA sequences in adjacent positions.

A model of viral transcription which incorporates this conclusion is diagrammed in Fig. 2 and described in detail in the legend. For the transcription to proceed to the 5′ end of the RNA and to reinitiate reproducibly at the 3′ end, it appears likely that there is an identical or near-identical terminal redundancy in the RNA. One important consequence of this model, however, is that one of the terminal repeats is lost during the transcription process (Fig. 2). One must therefore further postulate that the DNA provirus integrates in the cell in a region of the cellular genome also containing that sequence (e.g., in tandem with an endogenous virus sequence) so that it may be recovered on (DNA → RNA) transcription of the viral genome from the integrated sequence.

The DNA transcription products predicted by this model for the (−) strand are consistent with the homoduplex structures which were observed in these studies (Figs. 1 and 2). The two principal pathways to hybrid formation are represented in Fig. 2: the first involves an initial nucleation between the cDNA and central sequences of the RNA (*b* to *y*); the second involves an association between the 5′ terminal $a' + z'$ sequence of the cDNA and the 5′ terminal $a + z$ sequence of the RNA. The former nucleation event initially yields a linear duplex, which can in turn serve as intermediate in the formation of circles or dimers. The latter nucleation event leads directly to the formation of circles. The distance from the 4S primer to the 5′ end of the genome ($z + a$ in Fig. 2) has been estimated to be about 100 nucleotides (17) or about 1% of the viral genome. If the initial nucleation rate is proportional to the number of nucleotides available, then the second route (leading to circle formation) should account for about 1% of all hybrids; the pathway involving linear duplexes should account for formation of the remaining 99% of hybrids.

Circle formation through the major pathway involving linear intermediates as represented in Fig. 2 can occur only if a unique sequence (z) from the 5′ end of the RNA is represented in the initial DNA transcript. These sequences (z and z') serve as sticky ends for the linear duplex and would normally be expected to undergo pairing (if greater than approximately 20 nucleotides in length) to result in circularization of the hybrid. Due to the difficulty of interpreting those heteroduplex structures which were tangled and the uncertainty that RNA in linear heteroduplex molecules was absolutely full length (thereby possibly over-estimating the number of full length duplexes), it is not possible to estimate precisely the relative frequencies of circular molecules and full-length linear molecules. However, in one test approximately 50% (9/18) of interpretable genome length duplex molecules were circular. Although this is lower than what would be expected *a priori* from circularization of linear molecules in the diagram of Fig. 2, we are unsure of the stability of short base-paired regions during the glyoxal incubation and in spreading from 40% formamide; circles which had formed during the hybridization may have been opened into linear forms by these subsequent treatments. If the region from the primer to the 5′ end of the RNA were instead totally redundant (i.e., $z = 0$) rather than partially unique, then the linear duplexes would have no sticky ends, and circle formation could take place only through the second (minor) pathway. In this case, circles would be only about 1% of the frequency of full-length linear duplexes. The higher observed frequencies of circles would be hard to reconcile with this model, and must be considered evidence against the suggestion (18) that the entire region from the 4S primer to the 5′ terminus is duplicated at the 3′ end of the viral genome.

It should also be mentioned that we often see what appears to be a small tab of 110 ± 40 nucleotides in linear hybrids at a position 305 ± 50 nucleotides from the SV40 molecules (inset, Fig. 4), and thus approximately where the poly(A) joins the heteropolymeric sequences of the viral genome (see above). This corresponds with the expected location of an unhybridized z' sequence at the 5′ end of the DNA (Fig. 2), and gives an approximate estimate of its length. This tab would not be expected unless it contained a nonredundant sequence. The tab is also observed in hybrids spread from the weakly denaturing (U+F) solvent without prior glyoxal incubation and in the absence of SV40-poly(dT). Hence, the tab is not an artifact attributable to glyoxal-induced end denaturation or unusually long poly(dT) tails on SV40 in the poly(A) mapping. The observation of the tab thus lends further support to the model in which the region

of RNA from the 4S primer to the 5′ terminus is at least partially unique. This model is firmly supported by sequencing data (W. Haseltine, J. Coffin, A. Maxam, W. Gilbert, L. Weith, and D. Schwartz, personal communication) which were communicated to us after our experiments and data analysis were concluded.

The molecular size of the RSV hybrids of 9.70 ± 0.57 kilobases corresponds closely with other estimates of 35S genome size by sedimentation (4), gel electrophoresis (19), and electron microscopy (20, 21).

We have shown directly by electron microscopy that the transformation defective mutants of the nondefective sarcoma viruses studied here (Pr-B and Pr-C) are deletion mutants. The sizes and positions of the deletions are estimated as 1.97 ± 0.21 kb for td-Pr-B, extending from 0.86 ± 0.10 to 2.83 ± 0.23 kb of the nondefective Pr-B genome; and 2.38 ± 0.27 kb for td-Pr-C, extending from 0.73 ± 0.21 to 3.11 ± 0.34 kb of the nondefective Pr-C genome. Although these figures show that differences are small between the *td* deletions of Pr-B and Pr-C, the differences were judged to be greater than could be explained by experimental error. These heteroduplex results correspond well with earlier studies by other techniques which had implied that the transformation defective viruses were probably deletion mutants. The extent of the deletion was estimated to be 12–24% by gel electrophoresis (19) and 16–20% by hybridization (22, 23); the site of the deletion was judged to be near the 3′ end of the RNA by fingerprint analysis of poly(A)-tagged fragments (24, 25).

Heteroduplexes between Pr-B cDNA and Pr-C RNA showed no regions of nonhomology between them. Though genetically closely related, there are differences between the viruses, both serologically and in the detail of their nucleotide sequences in the glycoprotein regions of the genomes (14, 23, 24). This case serves as an example of the limitations of the heteroduplex method as applied to genetic analysis. To discern a region of nonhomology between nucleic acid pairs by the present heteroduplex technique, the region of nonhomology must be at least 100 nucleotides in length (1). It is certain then that mismatches occur in the Pr-B·Pr-C heteroduplex, but they apparently are well enough interspersed with homologous sequences that the sites of nonhomology are not identifiable.

We wish to acknowledge the expert technical assistance of Valerie Ng and Yu-Sun Liu. We thank Peter Duesberg for his interest and valuable discussions as well as for supplying cells and viruses. We wish to thank Welcome Bender for critical reading of the manuscript prior to publication and William Haseltine and Harold Varmus for sharing unpublished data with us. The major portion of the electron microscopy was performed by one of the authors (S.H.). R.J. is a post-doctoral fellow of the Helen Hay Whitney Society. This work was supported by Grant no. AI 00634 from the National Institute of Allergy and Infectious Diseases (to C.A.K.) and by Contract NO-1-CP-43306 with the Virus Cancer Program of the National Cancer Institute (to N.D.).

1. Davis, R., Simon, M. & Davidson, N. (1971) *Methods Enzymol.* **21D,** 413–428.
2. Green, M. & Gerard, G. (1974) *Prog. Nucleic Acid Res. Mol. Biol.* **14,** 187–334.
3. Junghans, R., Duesberg, P. & Knight, C. (1975) *Proc. Natl. Acad. Sci. USA* **72,** 4895–4899.
4. Duesberg, P. (1970) *Curr. Top. Microbiol. Immunol.* **51,** 79–104.
5. Bishop, J. (1972) *Biochem. J.* **126,** 171–185.
6. Bender, W. & Davidson, N. (1976) *Cell* **7,** 595–607.
7. Lee, C., Davis, R. & Davidson, N. (1970) *J. Mol. Biol.* **48,** 1–22.
8. Junghans, R. (1975) Ph.D. Dissertation, University of California, Berkeley (University Microfilms, Inc., Ann Arbor, Mich.).
9. Leis, J., Berkower, I. & Hurwitz, J. (1973) *Proc. Natl. Acad. Sci. USA* **70,** 466–470.
10. Verma, I. (1975) *J. Virol.* **15,** 843–854.
11. Wang, L. & Duesberg, P. (1974) *J. Virol.* **14,** 1515–1529.
12. Vogt, P. (1971) *Virology* **46,** 939–946.
13. Duesberg, P. & Vogt, P. (1973) *Virology* **54,** 207–219.
14. Duff, R. & Vogt, P. (1969) *Virology* **39,** 18–30.
15. Wellauer, P. & Dawid, I. (1973) *Proc. Natl. Acad. Sci. USA* **70,** 2827–2831.
16. Taylor, J. & Illmensee, R. (1975) *J. Virol.* **16,** 553–558.
17. Haseltine, W., Kleid, D., Panet, A., Rothenberg, e. & Baltimore, D. (1976) *J. Mol. Biol.* **106,** 109–131.
18. Collett, M. & Faras, A. (1976) *Proc. Natl. Acad. Sci. USA* **73,** 1329–1332.
19. Duesberg, P. & Vogt, P. (1973) *J. Virol.* **12,** 594–599.
20. Mangel, W., Delius, H. & Duesberg, P. (1974) *Proc. Natl. Acad. Sci. USA* **71,** 4541–4545.
21. Kung, H., Bailey, J., Davidson, N., Vogt, P., Nicolson, M. & McAllister, R. (1974) *Cold Spring Harbor Symp. Quant. Biol.* **39,** 827–834.
22. Stehelin, D., Guntaka, R., Varmus, H. & Bishop, J. (1976) *J. Mol. Biol.* **101,** 349–365.
23. Tal, J., Fujita, D., Kawai, S., Varmus, H. & Bishop, J. (1977) *J. Virol.*, in press.
24. Wang, L., Duesberg, P., Beemon, K. & Vogt, P. (1975) *J. Virol.* **16,** 1051–1070.
25. Coffin, J. & Billeter, M. (1976) *J. Mol. Biol.* **100,** 293–318.